IEEE Access
Multidisciplinary | Rapid Review | Open Access Journal

Received May 22, 2021, accepted July 26, 2021, date of publication August 9, 2021, date of current version August 16, 2021.

Digital Object Identifier 10.1109/ACCESS.2021.3103438

Musculoskeletal Model to Predict Muscle Activity During Upper Limb Movement

YOKHESH K. TAMILSELVAM[1], JACKY GANGULY[2], RAJNI V. PATEL[3,†], (Life Fellow, IEEE), AND MANDAR JOG[4,†], (Member, IEEE)

[1]Canadian Surgical Technologies and Advanced Robotics (CSTAR), Department of Electrical and Computer Engineering, University of Western Ontario (UWO), London, ON N6A 5B9, Canada
[2]London Movement Disorders Centre, London, ON N6A 5A5, Canada
[3]Canadian Surgical Technologies and Advanced Robotics (CSTAR), Department of Surgery, Department of Clinical Neurological Sciences, Department of Electrical and Computer Engineering, University of Western Ontario (UWO), London, ON N6A 5B9, Canada
[4]London Movement Disorders Centre, Department of Clinical Neurological Sciences, University of Western Ontario (UWO), London, ON N6A 5A5, Canada

Corresponding author: Yokhesh K. Tamilselvam (ykrishn4@uwo.ca)

[†]Project Co-leader

This work was supported by the Mitacs Accelerate Research Grant.

This work involved human subjects or animals in its research. Approval of all ethical and experimental procedures and protocols was granted by the Office of Human Research Ethics, in Western University's Research Ethics Boards (REB) under the protocol number 108252.

ABSTRACT Assessing biomechanics of upper limb movement is essential for guiding targeted therapy to treat conditions such as spasticity and dystonia. Targeted therapy, including injections of medications into specific muscles (e.g., lidocaine, botulinum toxin type A), requires accurate identification (activity) and contribution of as many muscles as possible. Currently, this is achieved by visual clinical assessment or using surface electromyography (sEMG). Although sEMG could provide a reasonable estimate of muscle activity for certain superficial muscles after an intense filtering process, they are unable to provide separated activity and contribution for every superficial and deep muscle. Other proposed musculoskeletal and machine learning models similarly do not provide a detailed and accurate activity of every muscle. The objective of the study is to design a subject-specific musculoskeletal model to predict the activity and contribution of each muscle pertaining to any upper limb movement with improved detail and accuracy over existing methodologies. Performance metrics were calculated for validation by comparing the predicted muscle activity with the normalized sEMG data computed from 8 superficial muscles, while the deeper muscles were not included in the validation as the sEMG is unable to provide a separated activity for those muscles. The results show that the proposed model has a mean R^2 value of 0.8190 and also indicated a statistically significant correlation ($P < 0.0001$) between the calculated (normalized sEMG data) and predicted activity value. Additionally, and significantly, compared to earlier studies, the proposed model predicts the individual muscle activity and contribution of deeper muscles.

INDEX TERMS Muscle activity prediction, musculoskeletal model, simulation, subject-specific analysis, upper-limb.

I. INTRODUCTION

Multi-segmental upper limb movements are complex as each joint is controlled by many superficial and deep muscles and can have multiple degrees of freedom. The complexity makes it difficult to accurately determine the activity and relative contribution of each muscle to overall limb motion. With advances in the treatment of conditions such as dystonia, tremor, and spasticity using targeted intramuscular injection therapies (e.g., botulinum toxin), there is a potential need to better model muscle activity and its contribution to upper limb joint motions. This is because the therapeutic efficacy depends on proper targeting and dosage determination of muscles for which knowledge of the exact activity and contributions of individual muscles is required. However, such detailed modeling of muscle activity and contribution for upper limb motion is lacking, which is the motivation behind this study. Currently, methods for determining muscle activity involve visual assessment and surface EMG (sEMG) [1]. sEMG is the standard method used by clinicians to determine

The associate editor coordinating the review of this manuscript and approving it for publication was Seok-Bum Ko.

the muscle activity as simultaneous, multi-muscle intramuscular needle EMG is highly invasive, painful, and in some cases, the patient needs to be anesthetized [2]. Hence, the only clinically used objective measuring technique is sEMG, which provides a compound muscle activity value only for some of the superficial muscles and is unable to provide the activity of deeper muscles [3], [4]. Additionally, the sEMG activity calculated for superficial muscles is affected due to mechanical and motion artifacts and therefore requires proper positioning of the sensor and various filtering techniques to remove any noise signals [5], [6]. Moreover, sEMG tells us the activity of muscles individually but does not provide an overall relative contribution of each muscle as it cannot determine the passive force of the muscles. Using sEMG and kinematic measures of limb movements, other musculoskeletal models [7], [8] and machine learning methods [9] have also been proposed to predict muscle contribution to motion. However, there are numerous limitations in the existing models such as lack of detail (only a few muscles were considered leaving out remaining muscles which could also remain active to perform the desired movement), no subject-specific modeling, and lower prediction accuracy when compared with calculated sEMG value for superficial muscles. Therefore, there is currently a need to develop a more accurate, detailed, and subject-specific method to predict muscle activity/ contribution to a desired upper limb motion [10]. To define some of the terminologies, muscle force can be divided into active force (that associated with actin-myosin cross-bridge) and passive force (tension arising in the muscle's elastic element when stretched) [11]. This study refers to two different muscle parameters: muscle activity and muscle contribution, computed using the muscle's active and passive force. Muscle activity is determined by the active force generated by the individual muscle, comparable to sEMG data. In contrast, muscle contribution involves active and passive force and is calculated as a relative percentage of all superficial, deep, and smaller muscles performing and maintaining a joint movement/position.

This work proposes a detailed subject-specific model that includes all the superficial and deep muscles capable of performing multi-joint upper limb motions. The proposed musculoskeletal model was developed using The AnyBody Modeling System^{TM} (AMS^{TM}) (Version 7.2.3, AnyBody Technology) [12]. The model takes kinematic motion data as inputs and outputs the force and kinematic data of the individual arm muscles. The model includes 61 upper-limb muscles containing 141 muscle elements, 7 rigid bone elements, and 7 functional joints, making the model much more detailed than earlier studies. Validation of the model's performance was done through comparisons with normalized sEMG data as it is currently the standard tool used by clinicians and is considered the gold standard for determining muscle activity. Performance metrics such as R^2, Root Mean Squared Error (RMSE), and significance of correlation coefficient were calculated between the predicted and calculated (normalized sEMG) activity data. These performance metrics showed a higher correlation for superficial muscles than previous models indicating a more accurate prediction which is one of the primary contributions of this study. In addition to being more detailed and accurate than earlier models, the proposed model is also subject-specific as most parameters associated with rigid bone, muscle, and joint elements can be adjusted to fit the subject. Furthermore, the study also estimates the individual muscle contribution, which has not been done in earlier studies.

II. METHODS

A. SUBJECTS

Six healthy subjects (age - mean: 28 years; range: 25-32 years, mass - mean: 81.5 kg; range: 72-87 kg, height - mean: 1.72 m; range: 1.66-1.85 m) participated in this study. The Office of Human Research Ethics, in Western University's Research Ethics Boards (REB), approved this study protocol (protocol number: 108252). All subjects provided their informed consent approved by REB prior to the study. This study analyzed only the movements of the right arm, and the participants were asked to perform five distinct sets of tasks. Each task comprised a multitude of movements involving three upper extremity joints (wrist, elbow, and shoulder). The subjects were asked to perform five trials for each of the tasks.

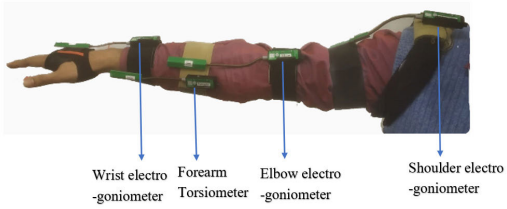

FIGURE 1. Sensor placement.

TABLE 1. Sensor placements during kinematic data acquisition.

Sensor	Placement
Wrist electro goniometer	Posterior side of arm: third metacarpal and midline of the forearm
Forearm torsiometer	Anterior side of the forearm: mid-region of the forearm
Elbow electro goniometer	Exterior side of the elbow: upper end of the forearm and lower end of the humerus
Shoulder electro goniometer	Exterior side of shoulder: right over the deltoid muscle and between the shoulder point and neck joint

B. KINEMATIC DATA ACQUISITION

In this study, the arm movement was captured using wireless motion sensors, which were used as inputs to the model. Five

sets of tasks that involved a combination of joint movement in available Degrees of Freedom (DOF) were selected. Three electro goniometers [13] were used for measuring the joint angles about a movement in the wrist, elbow, and shoulder joints. Further, one torsiometer was used for measuring angles pertaining to the pronation/supination of the forearm. A detailed diagram indicating the location of the sensor in the arm is shown in Figure 1. A view from another plane is also provided in section II of the Supplementary Material to better indicate the exact position of the sensor. The data collected from the sensors were independent of each other, i.e., they are mutually exclusive [14]. Table 1 indicates the placement of each sensor on the arm.

1) DATA PRE-PROCESSING

The sensor data needed to be pre-processed before it could be provided as an input to the model. First, the sensor data were filtered using a high pass filter to avoid noise interference. The filtered data are then pre-processed using Python 3.5. For almost all the joint angles, there are some minor offsets between the sensor values and the values that need to be entered into the simulation model. For instance, a fully flexed wrist in the simulation model is -90 degrees, and a fully extended elbow in the simulation model is 90 degrees. However, the range of values in the sensors for the same movement is different. For instance, the sensor value for a fully flexed wrist is -50 degrees, and the sensor value for a fully extended elbow is 130 degrees. So, the range of values obtained from the sensors was converted to the range of values accepted by the simulation model while maintaining the ratio. One final step is to perform an interpolation operation. The interpolation increases the sample points by estimating the intermediate values. This would be useful in breaking down a motion into more steps and thereby allowing an in-depth analysis. Therefore, these corrected sensor values were then interpolated using the B-spline function of order four as it provides a smooth approximation of data points [15], [16]. Table 2 shows the joint angles associated with the respective movements. The value zero represents the joint angle when the arm is placed at the neutral or resting position while standing.

TABLE 2. Range of joint angles.

Movements	Joint angles (degrees)
Shoulder flexion/extension	-180 to 180
Shoulder abduction/adduction	0 to 180
Elbow flexion/extension	0 to 180
Forearm supination/pronation	-90 to 90
Wrist flexion/extension	-90 to 90
Wrist abduction/adduction	20 to -20

2) SEQUENCE OF JOINT MOVEMENTS INVOLVED IN THE TASKS

This section explains the sequence of joint movements performed in each task (see Table 3). Figure 2 shows the kinematic sensor data pertaining to task - 1, while the kinematic data for the other tasks are provided in the Supplementary Material (Figure S5, S8, S11, S14). The values in Table 2 can be compared with Figure 2 to identify the respective joint movements. The dotted lines divide the data into sectors depending on the timed change of the movement. For instance, the first sector does not have any voluntary joint movements, followed by the second sector, which indicates a voluntary shoulder flexion and so on. This sector-wise division was also carried out in the predicted and the calculated activity value to analyze the performance of the model. The methodology behind calculating the performance metrics using these divided sectors is explained in subsequent sections (Section II H).

TABLE 3. Sequence of movements associated with the task.

	Movement sequence
Task 1	Shoulder flexion to 90 degrees with the fully supinated forearm – elbow flexion to 90 degrees – Maximum wrist flexion – Maximum Wrist extension– Neutral wrist position– Elbow extension (neutral elbow position) - Shoulder extension (neutral shoulder position)
Task 2	Elbow flexion to 90 degrees with the fully supinated forearm– Forearm semi-pronation – Maximum forearm supination – Elbow extension (neutral elbow position)
Task 3	Shoulder abduction to 90 degrees with neutral forearm position – Maximum forearm supination – Maximum wrist abduction – Maximum wrist adduction – Neural wrist position – Neutral forearm position (Semi-prone) – Shoulder adduction (neutral shoulder position)
Task 4	Shoulder abduction to 90 degrees with the fully supinated forearm – Wrist rotation – Shoulder adduction (neutral shoulder position)
Task 5	Elbow flexion to 90 degrees with neutral forearm position - Shoulder abduction to 90 degrees – Maximum wrist flexion – Neutral wrist position – Shoulder adduction (neutral shoulder position) – Elbow extension (neutral elbow position)

While the five primary tasks only involve the three joints and their rigid bodies, other rigid bodies such as scapula and clavicle were also modeled. Joint movements pertaining to these rigid bodies were not included in the five tasks because these joint movements are usually not affected by the upper-limb tremor. Therefore, to address this limitation, a secondary result that involves muscle activity pertaining to scapula and clavicle motion such as shoulder protraction/retraction and shoulder elevation/depression was provided in section VII of the Supplementary Material.

C. SURFACE EMG: DATA COLLECTION AND PROCESSING

In this study, a Delsys Multi-contact sEMG sensor has been used to collect data for the five-set of tasks described

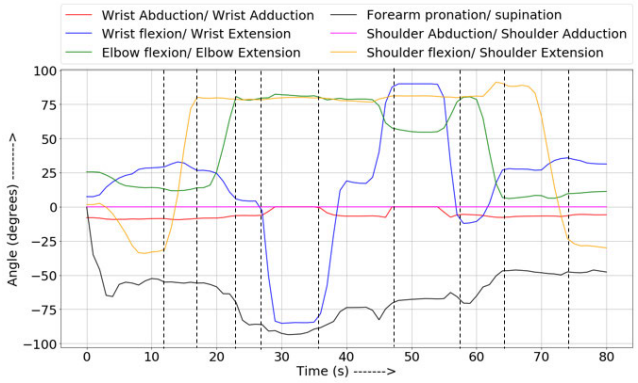

FIGURE 2. Motion data obtained from sensors after pre-processing for task - 1.

in Table 3. The sEMG data were recorded simultaneously during the kinematic data acquisition to ensure that the kinematic data and sEMG data correspond to the exact same motion. The sEMG activity has been calculated for 8 superficial muscles involved in upper extremity movements: Biceps, Triceps, Flexor Carpi Radialis (FCR), Extensor Carpi Radialis (ECR), Deltoid, Teres Major, Pectoralis Major, Latissimus Dorsi. The sEMG suffers from various limitations mentioned earlier. Therefore, to minimize the effect of these limitations and get a better estimate, sEMG recordings were collected over five trials for every task. These five trials were then averaged together to avoid any signal noise. Moreover, steps were taken to ensure that the sEMG sensor was placed over the proper muscle belly to avoid muscle crosstalk. In order to avoid noise and extract the necessary information, the sampling rate was chosen to be 1000 Hz. A study by Ives and Wigglesworth [17] has determined the appropriate sampling rate for sEMG data acquisition. This study has indicated that under-sampling could lead to loss of information, and oversampling above 1000 Hz is not necessary to capture the critical aspects of the sEMG signal. Therefore, 1000 Hz is usually the recommended sampling rate for the sEMG to capture the necessary information. The sEMG data were rectified and filtered using a second-order Butterworth filter with a cut-off frequency of 20 Hz. The sEMG data were also collected for all the 8 superficial muscles during the corresponding Maximum Voluntary Contraction (MVC), which was then used to normalize the obtained sEMG recordings.

The normalized sEMG data for the 8 superficial muscles were then compared with their corresponding predicted value to calculate the performance metrics such as Root Mean Squared Error (RMSE), R^2, and p-value to determine and validate the efficacy of the proposed model. The performance metrics were calculated only for superficial muscles as the sEMG does not provide activity data for deep muscles.

D. MUSCULOSKELETAL MODEL

This section provides the general method used in designing the musculoskeletal model. The methodology applied in transforming this model into subject-specific is provided in the next subsection. Figure S1. in the Supplementary Material shows the musculoskeletal model used in this study.

1) RIGID BODY (BONES)

The bones associated with the shoulder, elbow, and wrist movements were modeled separately, whereas the bones associated with the hand were modeled as one single element without joints. The rigid bodies that compose the musculoskeletal model are the thorax, scapula, clavicle, humerus, radius, ulna, and hand. The bones are a rigid body element whose position and orientation are defined by.

$$q_i = \begin{bmatrix} r_i^T & p_i^T \end{bmatrix} \tag{1}$$

where r_i^T is the global position vector of the center of mass and p_i^T is a vector of the Euler parameters corresponding to the i^{th} rigid-body element.

2) JOINTS

Joints add constraints to the bones and thereby restrict their degrees of freedom (DOF). The kinematic constraints imposed by the joints were solved using the Newton Raphson method to perform a kinematic analysis. The functional joints of the proposed model are the wrist, elbow, radioulnar (forearm), glenohumeral (shoulder), scapulothoracic, acromioclavicular and sternoclavicular joint. In order to individualize each DOF allowed by a joint, the software considers each DOF separately using a driver object. This is done to account for their respective kinematic measures and perform movements in each DOF allowed by the joint independently. Therefore, one joint could have multiple driver objects depending on its degrees of freedom, and each of the modeled joints is moved using multiple driver objects to perform tasks in their available DOFs. For instance, the shoulder joint has three DOFs, namely a) flexion/extension, b) internal/external rotation c) abduction/adduction. While the shoulder joint is mechanically modeled as a ball and socket joint, in order to individualize each DOF, three different driver objects are programmed with each dedicated to one DOF and perform any action in that DOF. This dedicated driver object will consider the kinematic measures for that DOF, and the trajectories for each DOF have to be provided to their corresponding driver object. Therefore, the shoulder joint in this study is capable of performing any movement in the available three DOFs.

3) MUSCLES

Muscles are complicated mechanical units that enable the movements of the rigid body elements by contraction. The creation and working of muscle fibers are discussed in [18]. The study uses a three-component muscle model and considers the muscle as an elastic string wound around a rigid-body element. The study uses two different muscle types: via point muscle and wrapping muscle, depending on functionality and pathway. The proposed model includes 61 upper-limb muscles containing 141 muscle elements.

E. SUBJECT SPECIFIC MODELING

A general upper extremity model was constructed based on the method provided in Section II D. This model was then adapted to fit the participant from whom the kinematic data of upper extremity movement was obtained. Parameters related to three elements of the model, namely bones, joints, and muscles, were adjusted to fit the subjects.

1) ADAPTING THE RIGID BODY (BONES) PARAMETERS

In terms of rigid body elements, the model parameters such as length, mass, and inertia of the rigid body have been adjusted depending on the subject. The moment of inertia of the rigid body is indicated using an inertia tensor matrix shown in equation 2.

$$I = \begin{bmatrix} I_{xx} & 0 & 0 \\ 0 & I_{yy} & 0 \\ 0 & 0 & I_{zz} \end{bmatrix} \tag{2}$$

$$I_{xx} = I_{zz} = I_{yy} = f(Mass, radius, length) \tag{3}$$

The length of the rigid body is changed depending on the subject's arm length, while the mass of each rigid body segment is calculated as a percentage of body mass measured from the subject. The percentage associated with each rigid body for calculating its mass was obtained from earlier literature [19], [20]. The radius of the bone was also calculated separately using the measured length and mass. As the moment of inertia is a function of length, radius, and mass, the inertia tensor matrix also varies for each participant. The average rigid-body parameters assigned to the model are provided in section IV of the Supplementary Material.

2) ADAPTING THE JOINT PARAMETERS

The joints in the proposed model are kept constant because all the subjects involved in this study are healthy and had no joint disorders. Therefore, no adjustments in terms of joint parameters were required for this study. However, the constraints added by the joints could also be altered if the range of joint movement is affected due to any joint dysfunctions. Although it has not been shown in this study, the joint constraints have been altered in our trial runs to vary the joint mobility in attempting to fit the model to various joint dysfunctions such as those due to accidents and stress injury. The joint parameters are provided in section IV of the Supplementary Material.

3) ADAPTING THE MUSCLE PARAMETERS

For each muscle, the origin, via, and insertion points are user-defined and can be adjusted depending on the subject. In this study, the insertion points of muscles are changed to suit the bone length of the subject. The muscle path, insertion, and origin points can be altered to suit the subject if they suffer from any neuromuscular disorder. Theoretically, subject-specific Physiological Cross-Sectional Area (PCSA) can also be measured as a ratio of muscle volume and fiber length, which could provide us with a model that fits the subjects even more accurately. However, calculating the muscle volume and PCSA for each subject requires procedures like Magnetic Resonance Imaging (MRI) which is time and cost-intensive. Further, it is unsuitable for the application aimed in this study as procedures like MRI is not carried out during targeted therapy to treat movement disorders. Therefore, PCSA for each muscle is kept constant for all subjects. The parameters assigned to each of the muscles are provided in section IV of the Supplementary Material, and these parameters are obtained from existing studies [21]–[24]. While these muscle parameters are kept constant for the five tasks performed by the six subjects, the model is capable of adapting the muscle parameters and predicting the activity accordingly. Therefore, to demonstrate this, three sets of muscle parameters are obtained from earlier studies [25], [26], and corresponding muscle activity for each set of muscle parameters was predicted for an elbow flexion/ extension. The results for this elbow motion with varying muscle parameters are given in section VI of the Supplementary Material.

F. MUSCLE RECRUITMENT DYNAMICS

1) INVERSE DYNAMICS IN THE MUSCULOSKELETAL MODEL

Biologically, the muscle recruitment process in a human body is carried out using activation dynamics [27], [28]. However, the musculoskeletal model used for this study does not include activation dynamics. This section explains how inverse dynamics replaces activation dynamics to predict the muscle forces and moments based on the kinematics and inertial forces. The inverse dynamics algorithm used in this study comprises an objective function that needs to be minimized to obtain the optimal force exerted by each muscle to complete a task. Equation 4 below shows the equilibrium equation for the musculoskeletal system:

$$Cf = r \tag{4}$$

where $f = [f(m) f(r)]^T$ is a vector containing the muscle force ($f(m)$) and joint reactions ($f(r)$). This is the unknown and needs to be determined. C is the coefficient matrix for the unknown forces, where each row in this matrix comprises coefficients to muscle forces pertaining to an element in the vector r. The values of these coefficients depend on the position of body segments at that instant. On the right-hand side of equation (4), r denotes the external and the inertia forces. The complication in solving for the vector f is that more than one muscle can move a joint, which means that there are more unknowns than equations in this system, which in turn indicates more than one solution for a specific kinematic arm configuration. Biologically, the central nervous system (CNS) uses a specific criterion in the activation dynamics to solve this redundancy and recruit the necessary muscles. Although the activation dynamics are not present in the proposed model, the criteria used for muscle recruitment in inverse dynamics need to resemble the CNS criteria. A previous study by Prilutsky and Gregor [29] discusses the performance of multiple objective functions that have been proposed to replicate the criterion used by the CNS to recruit muscles. Therefore, a similar objective function was used in

the inverse dynamics model for solving the redundancy and predicting the optimal muscle forces (f). The optimization problem is specified as follows [30].

$$Minimize\ G(f^{(M)}) \tag{5}$$

$$\text{Subject to } Cf = r \tag{6}$$

$$f_i^{(M)} \geq 0, \quad i = 1, 2, n \tag{7}$$

where G is the objective function to be minimized to obtain the optimal value of the vector f. The first constraint is the equilibrium equation, which enables us to take the motion kinematics into account. The second constraint is that the muscle force must always be non-negative as the muscles can only pull and not push. The chosen objective function (G) is shown in equation 8:

$$\mathrm{G} = \sum\nolimits_i \left(\frac{f_i^{(M)}}{N_i} \right)^P \tag{8}$$

where $f_i^{(M)}$ is the muscle force. The degree of the polynomial (P) was chosen as 3 based on previous literature [29], which indicates that an objective function with a third-degree polynomial was found to have the least error compared to others and further increases muscle synergism. A lower polynomial value discourages muscle synergism, whereas a higher polynomial might cause an abrupt change in contraction and elongation of a muscle, which is not physiologically possible. The strength of the corresponding muscle is taken as a normalization factor (N_i) to regularize the muscles with varying strength and thereby ensure that larger/stronger muscles carry more load than smaller/weaker muscles.

The proposed model considers the force-length-velocity relationship when predicting the muscle force for a task. Quental *et al.* [31] and Nikooyan *et al.* [32] have also implemented the force-length-velocity relationship in their upper-limb model. A comparison with these existing models is provided in the Discussion section. The N_i is a time-dependent muscle strength parameter that indicates the maximum force that a specific muscle can produce at a given instant. This parameter is a function of maximum muscle force, normalized force-length, and normalized force-velocity relationship. Therefore, the force-length-velocity relationship was considered through the normalization factor in equation 8. This normalization parameter also puts a limit on the maximum force that a muscle could generate through the variable F_0. The normalization parameter is shown in equation 9.

$$N_i = F_0 cos\,(\alpha)\,\widehat{F\,(l)}\widehat{F\,(v)} \tag{9}$$

where F_0 is the maximum isometric force, α is pennation angle, $\widehat{F\,(l)}$ is the normalized force-length relationship, and $\widehat{F\,(v)}$ is the normalized force-velocity relationship. The above-mentioned normalization parameter ensures that the resulting muscle force obtained from minimizing the objective function satisfies the force-velocity-length relationship.

G. MUSCLE ACTIVITY AND CONTRIBUTION

This section explains how the active, passive muscle force and muscle kinematics predicted from the proposed model were used to calculate the muscle activity and contribution.

1) MUSCLE ACTIVITY

Muscle activity is calculated using the muscle's active force involved in performing a movement and is comparable to the sEMG. The active force needs to be generated to complete a specific movement and is associated with the actin-myosin cross-bridge. For instance, the biceps and brachioradialis produce active force to perform elbow flexion, while the triceps and anconeus produce active force to perform elbow extension. This active force also depends on the load applied to a rigid body structure. There was no external load applied in this study but, gravity is compensated by simulating a load in the y-direction.

2) MUSCLE CONTRIBUTION

Muscle contribution indicates the share of contribution by each muscle in performing and maintaining the desired joint movement and position, respectively. It involves both the active and passive force of the muscle. The muscle activity parameter tells us the activity of a single muscle but does not tell us the contribution of a muscle compared to every other muscle involved in that movement. This value is provided in the muscle contribution in percentage. For instance, to maintain an elbow joint flexed at 90 degrees, a contribution of 30% from biceps, 40% from triceps, 10% from brachioradialis, and 20% from brachialis might be required. The contribution from primary muscles, when added up, does not practically come up to 100%, as some smaller muscles could also contribute to maintaining joint stability. This study will show the result of a set of superficial and deep/small muscles that are already known to contribute to specific joint movement. However, contributions from other muscles could also be obtained from our model. One of the advantages of the proposed model is that the active and passive force for smaller/ deeper muscles can be predicted, which provides us with enough information in calculating the exact contribution percentage of each muscle to a specific movement. In contrast, sEMG cannot quantify the passive force of the muscles.

3) ESTIMATION OF MUSCLE ACTIVITY AND CONTRIBUTION

The proposed model predicts the active and passive force through the inverse dynamics optimization explained earlier. The three-element muscle model that is used in this study, as shown in Figure 3 [33], consists of a contracting component (CC), a parallel elastic component (PEC), and a series elastic component (SEC).

The CC is the source of the muscle's active force (F_A), while the PEC and SEC represent the source of the muscle's passive behavior (F_P) and the elasticity of the tendon, respectively. The variable γ represents the pennation angle of the muscle, while L_m and L_t represent the length of the muscle's

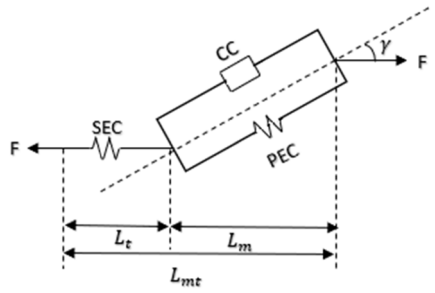

FIGURE 3. Three-element muscle model.

contractile element and the tendon, respectively. The individual muscle activity (MA) and muscle contribution (MC) in this study are calculated using the predicted muscle force as shown in equations 10 and 11, respectively.

$$MA_j = \frac{F_A^j}{F_{MVC}^j} \tag{10}$$

where F_{MVC} is the force at maximum voluntary contraction and F_A^j indicate the time-varying active force at j^{th} muscle.

$$MC_j = \frac{\left(\overline{F_p^j} + \overline{F_A^j}\cos\gamma^j\right) * PCSA^j}{\sum_{i=1}^{n}\left(\overline{F_p^i} + \overline{F_A^i}\cos\gamma^i\right) * PCSA^i} \tag{11}$$

where the terms $\overline{F_A^j}$ and $\overline{F_P^j}$ indicate the normalized active and passive forces generated by the j^{th} muscle respectively, the terms $\overline{F_A^i}$ and $\overline{F_P^i}$ present in the denominator indicate the normalized active and passive force generated by the i^{th} muscle respectively and $PCSA^j$, $PCSA^i$ are the Physiological Cross-Sectional Areas of the j^{th} and i^{th} muscle respectively. The force at the MVC (F_{MVC}) was obtained from the model for each muscle. All the values mentioned above except F_{MVC} and PCSA are time-dependent and continuous.

H. CALCULATING THE PERFORMANCE METRICS OF THE MODEL

The normalized sEMG data (See section II C) and the predicted activity value from the model (See section II G) were compared to calculate the performance metrics for determining the efficacy of the model. Before this calculation, the normalized sEMG data and predicted value were divided into sectors based on the timed change of the movement. These sectors were indicated through dotted lines in figure 2. Only the predicted output belonging to that sector were compared with the corresponding normalized sEMG output belonging to the same sector. This was done to ensure that the predicted and calculated data belonging to the different joint movements were not compared, leading to incorrect performance metrics. While the performance metrics were calculated for each sector separately, the RMSE for each muscle was obtained by averaging RMSE computed from each sector. The correlation (R) obtained from each sector were also combined together for each muscle using Fisher's Z-transformation method [34], [35]. Equations 12 and 13 indicate the generalized method for calculating the performance metrics such as RMSE and Pearson correlation (r).

$$RMSE = \sqrt{\overline{(MA_{EMG} - MA_{SIM})^2}} \tag{12}$$

$$r = \frac{\sum_{i=1}^{n}\left(MA_{EMG_i} - \overline{MA_{EMG}}\right)\left(MA_{SIM_i} - \overline{MA_{SIM}}\right)}{\sqrt{\sum_{i=1}^{n}\left(MA_{EMG_i} - \overline{MA_{EMG}}\right)^2}\sqrt{\sum_{i=1}^{n}\left(MA_{SIM_i} - \overline{MA_{SIM}}\right)^2}} \tag{13}$$

where MA_{EMG}, MA_{SIM} refers to the normalized sEMG and the predicted activity, respectively. A test to determine the significance of the correlation coefficient [36], [37] was performed for 8 superficial muscles in each sector, and a p-value for each of these tests was calculated. The p-value calculated for the 8 superficial muscles in each sector were combined using the harmonic mean method [38] to obtain a muscle-wise p-value. The null hypothesis when calculating the p-value is that the sEMG and predicted values are uncorrelated, which means if the p-value is less than our significance value (0.05), the null hypothesis could be rejected, providing us statistically significant evidence for the correlation between sEMG and predicted values. The calculated performance metrics are provided in the result section below.

III. RESULTS

A. OVERALL PREDICTED ACTIVITY AND CONTRIBUTION

The muscle activity and contribution described in equations 10 and 11 were calculated from the predictions of kinematics and force output obtained from the musculoskeletal model. Five trials were performed for every task, and the predictions were then averaged together to obtain a much more reliable output. Performing multiple trials of the same tasks ensures that the results are consistent and are not altered by any random events. To further generalize the result across multiple subjects, the activity and contribution output of the six subjects were also averaged together to obtain the final result. The overall muscle activity and contribution obtained through the proposed model for task 1 are shown in Figures 4 and 5, respectively, while the plots corresponding to the other tasks have been added in the Supplementary Material (Figure S6, S7, S9, S10, S12, S13, S15, S16). Muscle activity is dimensionless and ranges from 0 to 1, while the muscle contribution is represented in percentages. In addition to the superficial muscles, specific small, deeper muscles such as pronator teres, pronator quadratus, anconeus, brachialis, brachioradialis, and supinator are also analyzed as shown in Figure 6, some of which are not possible to estimate in an sEMG or using any previous models. A diagrammatic representation of the overall process involved in predicting the activity/contribution is provided in the Supplementary Material (Figure S4).

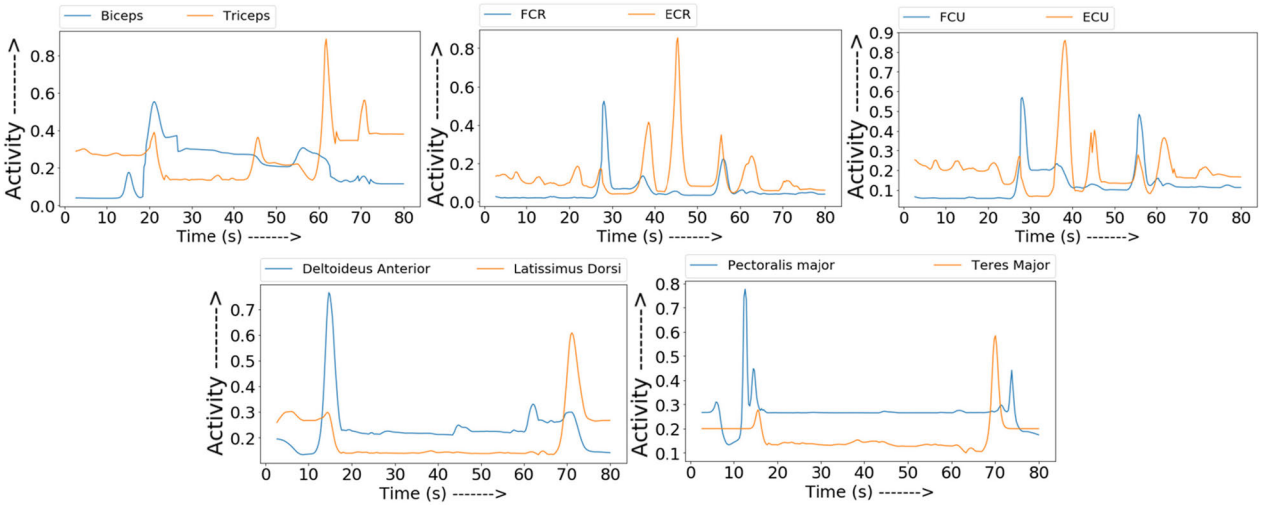

FIGURE 4. Overall muscle activity across six subjects through musculoskeletal model for task - 1.

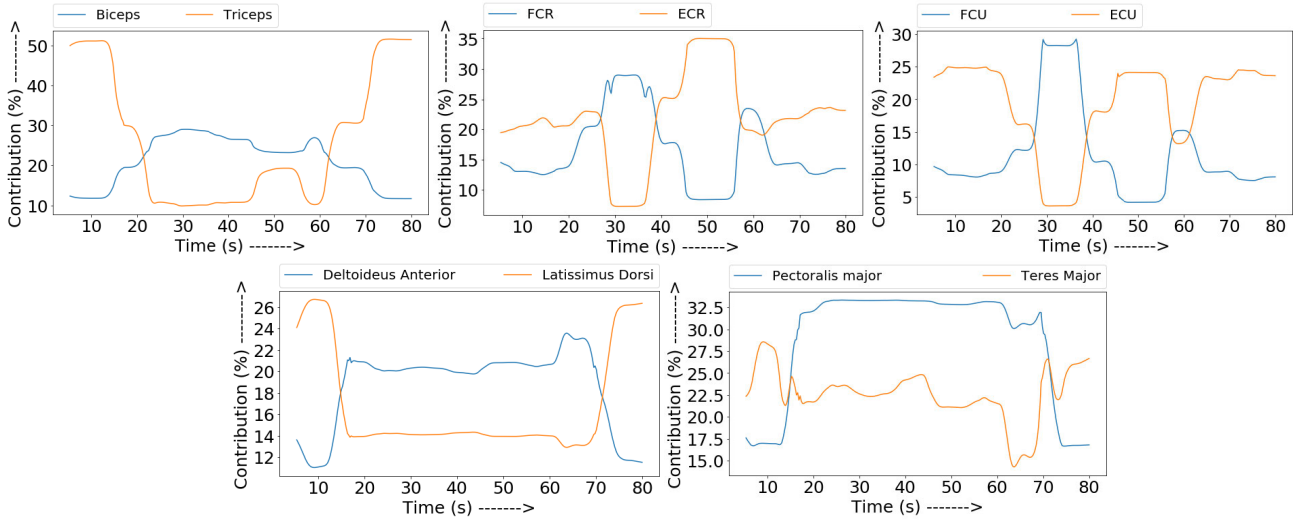

FIGURE 5. Overall muscle contribution across six subjects through musculoskeletal model for task-1.

B. SUBJECT-SPECIFIC ACTIVITY AND CONTRIBUTION

One of the study's goals was to obtain a subject-specific activity prediction. While the previous section indicated the intra-subject activity predictions (overall averaged activity across six subjects) for task 1, this section provides examples of the inter-subject predictions between two subjects.

The altered parameters are provided in section II E. Figure 7 shows the individual muscle activity for two subjects. In terms of measured and calculated parameters, the mass, length, and radius of the rigid body for subject-1 are approximately 15.9%, 8.95 %, and 3.15 % lower, respectively, than those for subject-2. The average principal axes of inertia (I_{xx}, I_{yy}, I_{zz}) are approximately 32.25 % lower for subject-1 than for subject-2. The muscle insertion and origin points were adjusted accordingly, while the joint constraints were the same for both subjects.

The activation of the two subjects almost aligns with each other even with varying parameters apart from increased activations in certain regions, which could be attributed to the higher inertia of the rigid body for that subject. This is because the predicted activity of each subject was normalized against the subject's corresponding activity at the muscle's MVC, which resulted in activity from multiple subjects to align with each other. The application of this subject-specific model would be more evident when used on patients with varying degrees of movement disorders or joint dysfunctions, which could help individualize the treatment based on the patient's condition. This subject-specific model contributes to that direction. Subsequent studies would focus on utilizing this subject-specific model using kinematic data collected from patients with movement disorders.

C. PERFORMANCE METRICS

Performance metrics were calculated by comparing our predicted output with the normalized sEMG output pertaining to the same movement. The procedure followed to acquire

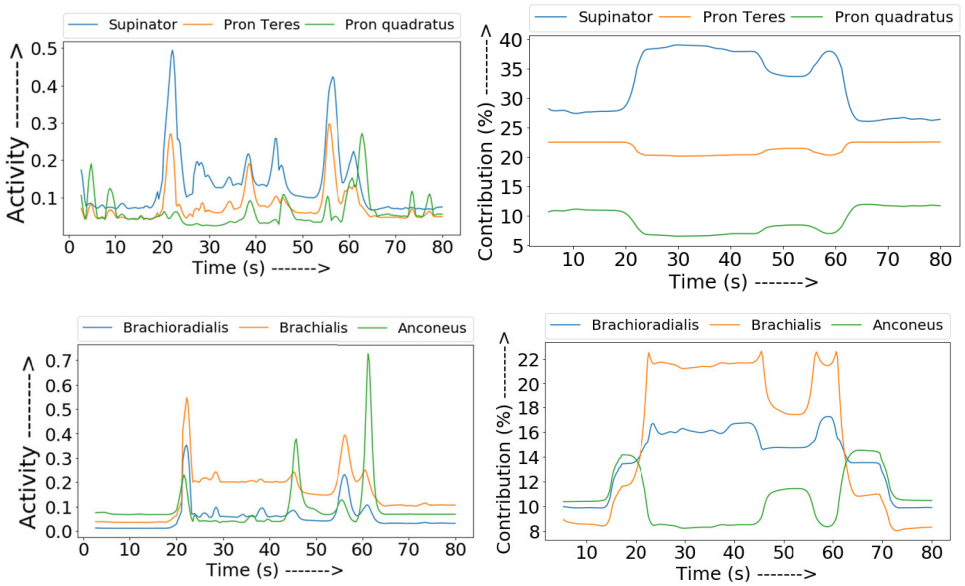

FIGURE 6. Overall muscle activity and contribution for smaller and deeper muscles for task-1.

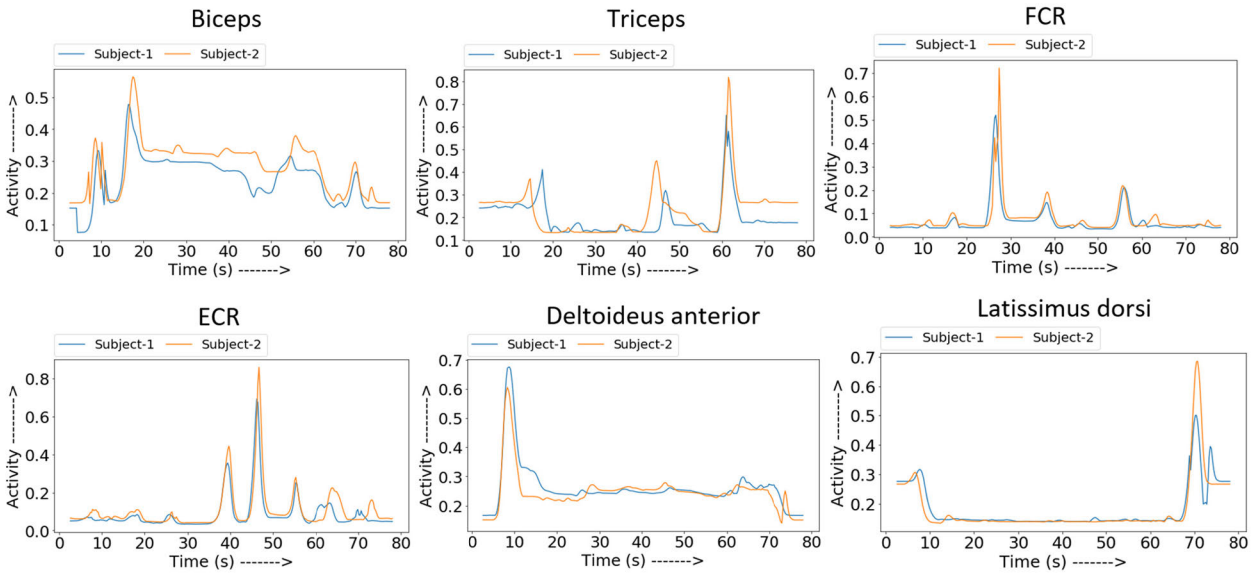

FIGURE 7. Muscle activity between two different subjects for task-1.

a reliable set of sEMG data for superficial muscles is mentioned in Section II C. Both the predicted output and calculated output are divided into sectors based on the timed change of movement and compared with their corresponding sector to estimate the performance metrics. Table 4 shows the performance metrics comparing the calculated and predicted activity values. The p-values that are below 10^{-10} are represented through a statement of inequality.

The average R^2 value across all the muscles was found to be 0.8190. The high R^2 value indicates a close correlation to the normalized sEMG data for the 8 superficial muscles. The RMSE average of our proposed model is 0.1031. There is a slight discrepancy between the predicted and calculated sEMG value leading to a small RMSE value. However, this small discrepancy can be justified. Even the sEMG recordings between multiple trials of the same movements could be slightly different. To confirm this, the RMSE value between sEMG recordings obtained from five different trials of the same movement was calculated and found to be 0.04485. Therefore, the obtained RMSE value for the proposed model is on the lower side, indicating that the predicted output closely resembles the normalized sEMG output for the 8 superficial muscles. Further, the overall p-value (in this case, the probability of an uncorrelated system) was

TABLE 4. Muscle-wise performance metrics of the model's activity output.

Muscle	Root Mean Squared Error (RMSE)	Pearson's correlation	Coefficient of Determination (R^2)	P-value
Biceps	0.014185	0.9297	0.8643	**< 0.0001**
Triceps	0.003462	0.8982	0.8067	**3.61e-09**
FCR	0.046810	0.8922	0.7715	**< 0.0001**
ECR	0.024805	0.9139	0.8352	**< 0.0001**
Deltoid	0.083255	0.9293	0.8635	**< 0.0001**
Latissimus dorsi	0.190851	0.9042	0.8175	**< 0.0001**
Teres Major	0.134105	0.8575	0.7353	**6.29e-08**
Pectoralis Major	0.327439	0.9034	0.8161	**< 0.0001**

calculated across the validated muscles mentioned in Table 4 using the harmonic mean method in order to control the family-wise error rate. The overall p-value was $P < 0.0001$, indicating that the correlation between the calculated and predicted value is statistically significant.

The obtained performance metrics indicate that the predictions of the proposed model align with the normalized sEMG data, which is currently considered the gold standard for calculating muscle activity. Although only 8 superficial muscles were used in calculating the performance metrics due to the limitation posed by sEMG, the proposed model also provides the activity of many more superficial and deep muscles. Further, our model can determine the exact contribution of each muscle in performing a movement.

Further validation can also be done by comparing Figure 2 for correlating the filtered sensor data to the corresponding activity or contribution plot. For instance, at t = 10s in task 1 (Figure 2), shoulder flexion took place and was matched by an increase in deltoideus activity and contribution shown in Figures 4 and 5, respectively. Furthermore, apart from superficial muscles, the activity of small/ deep muscles shown in Figure 6 could also be validated by comparing with the kinematic arm movement. For instance, at t = 20 s, an elbow flexion occurs, which is matched by an increase in the activity of brachialis and brachioradialis.

IV. DISCUSSION

The proposed work focuses on designing and adapting the developed model depending on the subject, i.e., developing a subject-specific model for analysis. Studies have stressed the importance of individualizing treatments provided for movement disorders to improve their effectiveness. In order to tailor the treatment based on the patient's condition, there is a need for a more accurate, detailed, and subject-specific analysis. While the earlier musculoskeletal models lack in this regard, the proposed model was designed to consider the various parameters that would affect the muscle activity/contribution pertaining to a motion. The musculoskeletal model uses kinematic motion data to predict muscle force, which is further used to determine muscle activity and contribution. The predicted activity was then compared with the normalized sEMG data corresponding to 8 superficial muscles to obtain the performance metrics, which indicated a good correlation. Our model and its performance metrics can also be compared with the existing models to indicate improved accuracy and detail.

A probabilistic model proposed by Johnson and Fuglevand [9] to predict activity for upper extremity muscles indicates an R^2 value of 0.40 ± 0.18 averaged across 12 different muscles when performing the movement in a three-dimensional space, which is significantly lower than the obtained R^2 value from the proposed model. Moreover, only 12 muscles were included in the probabilistic model lacking in detail. Klemt *et al.* [39] have proposed 10 MRI-based shoulder models containing 87 muscle elements. While this model is less detailed than the proposed model, the authors estimated muscle parameters using MRI on 10 subjects. However, the authors have indicated that this process is extremely time-intensive, and MRI is also not a technique that is used when treating patients with targeted therapies. Therefore, certain muscle parameters such as PCSA, optimal fiber length, muscle volume were not estimated in the study for each subject, although the model can predict muscle activity for varying muscle parameters. To showcase the model's ability to adjust muscle parameters based on a subject, the parameters have been altered based on already existing datasets obtained from earlier studies [25], [26], and the corresponding activity results for each set of parameters have been provided in section VI of the Supplementary Material. This indicates that the model can adjust to any subject's parameter and accurately predict muscle activity.

Wu *et al.* [40] have proposed another subject-specific model, but the model contains only 26 muscle-tendon units lacking in detail compared with the proposed model. Further, while the model's output was compared with other generic models, a correlation or RMSE value compared with the sEMG data was not computed. Therefore, the model's performance compared to the current gold standard technique for estimating muscle activity is unknown.

Another significant upper-limb model proposed by Nikooyan *et al.* is the Delft shoulder and elbow model [32] that can estimate muscle forces. Scaling of rigid bodies using this model [41] was also performed across two different subjects, which has resulted in improved accuracy.

TABLE 5. Comparison with earlier models.

	Performance metrics compared with sEMG	Model type	Muscles modeled	Functional joints	Rigid body
Proposed model	Correlation: 0.905 RMSE: 0.1031 R^2: 0.8190 $P < 0.0001$	Subject-specific	61 muscles and 141 muscle elements	7 functional joints: Wrist, elbow, radioulnar (forearm), glenohumeral (shoulder), acromioclavicular, scapulothoracic, and sternoclavicular joint.	7 rigid body segments: Humerus, Radius, Ulna, clavicle, scapula, hand, thorax.
Klemt et al. [39]	Average correlation of five muscle using Fisher's z transformation: 0.778	MRI based subject-specific	87 muscle elements	5 functional joints: Elbow, glenohumeral (shoulder), acromioclavicular and sternoclavicular joint.	6 rigid segments: Thorax, scapula, clavicle, humerus, radius, ulna
Nikooyan et al. [32] [41]	Correlation: 0.66	Subject-specific	31 muscles	5 functional joints: thoracic joints, shoulder girdle, glenohumeral, elbow, and wrist joint.	7 rigid segments: thorax, scapula, clavicle, Humerus, Radius, Ulna, hand
Quental et al. [43] [31]	Correlation: 0.90±0.05	Not subject-specific	22 muscles with 74 muscle elements	6 functional joints: sternoclavicular, acromioclavicular, glenohumeral, humeroulnar and radioulnar and scapulothoracic joints	7 rigid body segments: thorax, rib cage, clavicle, scapula, humerus, ulna, and radius
Wu et al. [40]	Correlation: Not computed	Subject-specific	26 muscles	4 functional joints: Elbow, glenohumeral, sternoclavicular, and acromioclavicular joints	5 rigid bodies: clavicle, scapula, thorax, humerus, and lower arm
Charlton et al. [47]	Correlation: Not computed	Not subject-specific	31 muscles	5 functional joints: sternoclavicular, acromioclavicular, glenohumeral, elbow and scapulothoracic	6 rigid body segments: thorax, clavicle, scapula, humerus, radius, and ulna
Pennestri et al. [8]	Correlation: Not computed	Not subject-specific	24 muscles	3 functional joints: glenohumeral, elbow, and wrist.	4 rigid body: Humerus, Ulna, radius, and hand

However, this model only considered the muscles pertaining to the shoulder and elbow, which includes about 31 muscles. A correlation with sEMG data was computed in [32] and was found to be 0.66. A study [42] was also conducted in which different scaling methods were compared to fit the shoulder model onto 30 volunteers. The result from the study indicates that it is possible to scale the model parameters to fit the subject. However, the muscle force or activity was not computed in this study, and therefore, the gain in accuracy due to the scaling approach was not indicated. Quental *et al.* [31] and [43] have proposed another comprehensive upper-limb model involving 22 muscles and includes all the functional joints except the wrist joint. The cross-correlation value computed between the predicted and sEMG value is 0.90, which is reasonably good. However, this model is not subject-specific and also lacks in detail with only 22 muscles. Further, the model considers short tendons to be rigid, which could affect the model's accuracy. Holzbaur *et al.* [25] have proposed a comprehensive musculoskeletal model containing 50 muscle compartments crossing multiple upper-limb joints. This model predicts muscle force but requires the pattern of muscle activations as input which could be challenging

to measure for many deep muscles, as mentioned in the introduction. However, this model estimates various muscle parameters over a wide range of postures, and some of these muscle parameters were used in our study.

The work by Buchanan *et al.* [44] aligns closely with our study and uses inverse dynamics to predict muscle forces and joint moments using the sEMG signal as input. This model does have a better R^2 value of 0.94 with the sEMG, but this model is driven using the sEMG input to calculate its parameters and therefore suffers from the same limitation as the sEMG mentioned earlier. Moreover, our proposed model has considerably more detail than the model in [44], where only four muscles were considered when calculating the parameters, and the remaining muscles were left out of the model. Further, considering that the sEMG data was the input and the output of the model has a higher correlation with the sEMG again, there is a possibility of the model overfitting to the input. Generalizing this model across multiple muscles could underfit the model leading to a significantly lower R^2 value. A lower limb model driven by Functional Electrical Stimulation (FES) was proposed by Cardona and García Cena [45], which can estimate the muscle length and moment arms. However, this model is also driven by the muscle activation signal, which is nearly similar to the earlier model driven by sEMG activity input leading to the same limitation as an sEMG-driven model. Several other models [7] and [46] were proposed, but they were either sEMG-driven, leading to similar shortcomings or lack in detail and accuracy. Table 5 compares the proposed model with some of the earlier upper-limb models.

Compared to earlier existing models or methodologies to measure/predict muscle activity, the proposed model has been shown to include a larger group of muscles, providing a much more extensive detail combined with a more accurate prediction. Additionally, the force-length-velocity relationship and elasticity of the tendon were also considered during predictions. Apart from accuracy and detail, previous work on musculoskeletal models does not distinguish between activity and contribution of the muscle. In contrast, the proposed model can provide an overall percentage of contribution as it can predict the active and passive force of even deeper muscles that could contribute to joint movement and stabilization. Moreover, many previous studies use a generalized model for all the subjects, while the proposed model can be adapted depending on the subject, which could also contribute to improvement in accuracy.

V. CONCLUSION

The objective of this paper was to present a methodology to accurately measure the muscle activity and contribution pertaining to an upper limb movement. The model's performance indicates a statistically significant correlation with the normalized sEMG data for 8 superficial muscles and better accuracy and detail than the existing musculoskeletal and machine learning models. The significance of the study is as follows: (1). The proposed model can predict the activity of smaller/ deeper muscles, which is not possible in sEMG and earlier models; (2). unlike intramuscular EMG, the proposed model is not invasive; (3). the proposed model is subject-specific; (4). The prediction accuracy compared to some earlier models is much higher; (5). the proposed model can calculate the individual muscle contribution for joint movement and stabilization.

However, there are a few limitations to the model that should be addressed in the future. Rigid bodies such as the hand and thorax have been modeled as one segment. However, biologically, there are 8 smaller rigid segments that make up the wrist bones which were not modeled separately. Further, finger joints (metacarpophalangeal, proximal interphalangeal, and distal interphalangeal joints) were not modeled; therefore, the proposed model cannot handle movements associated with finger joints.

Looking at the model's performance metrics, muscles such as pectoralis major and teres major have a higher RMSE value and lower correlation value, respectively. The difficulty is to pinpoint the exact source of the error as it could result from the model's prediction error or higher noise in the obtained sEMG data. One workaround is to use a more accurate method like intramuscular EMG to validate the predictions, although it is highly invasive and painful. Understanding the source of error could enable us to explore other objective functions or modeling techniques that could provide better predictions.

In the proposed model, the joints and rigid bodies associated with the scapula and the clavicle were modeled. The movements associated with these rigid bodies were simulated, and the results were provided in the Supplementary Material. However, this study did not measure kinematic data pertaining to the scapula and the clavicle bones directly from the subjects. The reasoning is that while the kinematic data associated with the humerus, radius, ulna, and hand are easier to collect using a wireless motion sensor, the kinematic data associated with the scapula and clavicle bones are much harder to obtain. Secondly, the upper-limb tremor usually doesn't affect rigid bodies and joints associated with the scapula or the clavicle. Therefore, it would not be essential to replicate their movements in the model. However, obtaining kinematic data associated with these rigid bodies from healthy or tremor subjects could enable us to perform a more in-depth analysis that might be required for a different application. Therefore, an extension of this study could focus on recording the scapula or clavicle movements from the subjects and using that data to drive the rigid bodies.

Finally, this musculoskeletal model was designed with a specific application in mind, which is the accurate muscle selection and dosage determination in targeted intramuscular injection therapies (e.g., botulinum toxin) for patients with tremors. The proposed model addresses this application by providing accurate and detailed predictions of individual muscle activity and contribution, which is necessary to target the muscle better and determine the injection dose. However, this model has not yet been used on any tremor patients,

and further work is needed to validate the model predictions for minor rhythmic motions. Therefore, adopting this model for the application mentioned above and predicting muscle parameters for tremor patients would be the primary focus for the immediate future.

REFERENCES

[1] A. I. Grigoriu, M. Dinomais, O. Rémy-Néris, and S. Brochard, "Impact of injection-guiding techniques on the effectiveness of botulinum toxin for the treatment of focal spasticity and dystonia: A systematic review," *Ann. Phys. Rehabil. Med.*, vol. 58, p. e79, Sep. 2015, doi: 10.1016/j.rehab.2015.07.193.

[2] R. H. Chowdhury, M. B. I. Reaz, M. A. B. M. Ali, A. A. A. Bakar, K. Chellappan, and T. G. Chang, "Surface electromyography signal processing and classification techniques," *Sensors*, vol. 13, no. 9, pp. 12431–12466, 2013, doi: 10.3390/s130912431.

[3] I. H. Lee, Y. C. Yoon, D. H. Sung, J. W. Kwon, and J. Y. Jung, "Initial experience with imaging-guided intramuscular botulinum toxin injection in patients with idiopathic cervical dystonia," *Amer. J. Roentgenol.*, vol. 192, no. 4, pp. 996–1001, Apr. 2009, doi: 10.2214/AJR.08.1535.

[4] D. H. Sung, J. Y. Choi, D.-H. Kim, E.-S. Kim, Y.-I. Son, Y.-S. Cho, S. J. Lee, K.-H. Lee, and B.-T. Kim, "Localization of dystonic muscles with 18F-FDG PET/CT in idiopathic cervical dystonia," *J. Nucl. Med.*, vol. 48, no. 11, pp. 1790–1795, Nov. 2007, doi: 10.2967/jnumed.107.044024.

[5] C. Disselhorst-Klug, T. Schmitz-Rode, and G. Rau, "Surface electromyography and muscle force: Limits in sEMG–force relationship and new approaches for applications," *Clin. Biomech.*, vol. 24, no. 3, pp. 225–235, Mar. 2009, doi: 10.1016/j.clinbiomech.2008.08.003.

[6] R. V. Miller, "Electromyography—Uses and limitations," *California Med.*, vol. 89, no. 4, pp. 250–252, 1958.

[7] M. Millard, T. Uchida, A. Seth, and S. L. Delp, "Flexing computational muscle: Modeling and simulation of musculotendon dynamics," *J. Biomech. Eng.*, vol. 135, no. 2, Feb. 2013, Art. no. 021005, doi: 10.1115/1.4023390.

[8] E. Pennestrì, R. Stefanelli, P. P. Valentini, and L. Vita, "Virtual musculoskeletal model for the biomechanical analysis of the upper limb," *J. Biomech.*, vol. 40, no. 6, pp. 1350–1361, Jan. 2007, doi: 10.1016/j.jbiomech.2006.05.013.

[9] L. A. Johnson and A. J. Fuglevand, "Evaluation of probabilistic methods to predict muscle activity: Implications for neuroprosthetics," *J. Neural Eng.*, vol. 6, no. 5, Oct. 2009, Art. no. 055008, doi: 10.1088/1741-2560/6/5/055008.

[10] B. Bolsterlee, D. H. E. J. Veeger, and E. K. Chadwick, "Clinical applications of musculoskeletal modelling for the shoulder and upper limb," *Med. Biol. Eng. Comput.*, vol. 51, no. 9, pp. 953–963, Sep. 2013, doi: 10.1007/s11517-013-1099-5.

[11] R. Zdero, M. M. Borkowski, and C. Coirault, "Measuring the contraction force, velocity, and length of skeletal muscle," in *Experimental Methods in Orthopaedic Biomechanics*. New York, NY, USA: Academic, 2017, pp. 363–378, doi: 10.1016/B978-0-12-803802-4.00023-8.

[12] J. Rasmussen, M. Damsgaard, E. Surma, S. T. Christensen, M. de Zee, and V. Vondrak, "AnyBody—A software system for ergonomic optimization," in *Proc. 5th World Congr. Struct. Multidiscip. Optim.*, May 2003, Venice, Italy, 2003, pp. 1–6.

[13] G. Legnani, B. Zappa, F. Casolo, R. Adamini, and P. L. Magnani, "A model of an electro-goniometer and its calibration for biomechanical applications," *Med. Eng. Phys.*, vol. 22, no. 10, pp. 711–722, 2000, doi: 10.1016/S1350-4533(01)00009-1.

[14] F. Rahimi, O. Samotus, J. Lee, and M. Jog, "Effective management of upper limb parkinsonian tremor by incobotulinumtoxina injections using sensor-based biomechanical patterns," *Tremor Other Hyperkinetic Movements*, vol. 2015, no. 1, pp. 1–13, 2015, doi: 10.7916/D8BP0270.

[15] H. Hou and H. Andrews, "Cubic splines for image interpolation and digital filtering," *IEEE Trans. Acoust., Speech, Signal Process.*, vol. ASSP-26, no. 6, pp. 508–517, Dec. 1978, doi: 10.1109/TASSP.1978.1163154.

[16] C.-C. Leung, P. C.-K. Kwok, K.-Y. Zee, and F. H.-Y. Chan, "B-spline interpolation for bend intra-oral radiographs," *Comput. Biol. Med.*, vol. 37, no. 11, pp. 1565–1571, Nov. 2007, doi: 10.1016/j.compbiomed.2007.02.004.

[17] J. C. Ives and J. K. Wigglesworth, "Sampling rate effects on surface EMG timing and amplitude measures," *Clin. Biomech.*, vol. 18, no. 6, pp. 543–552, 2003, doi: 10.1016/S0268-0033(03)00089-5.

[18] C. Gans, "Fiber architecture and muscle function," *Exerc. Sport Sci. Rev.*, vol. 10, no. 1, pp. 160–207, 1982, doi: 10.1249/00003677-198201000-00006.

[19] D. A. Winter, *Biomechanics and Motor Control of Human Movement*, 4th ed. Hoboken, NJ, USA: Wiley, 2009, doi: 10.1002/9780470549148.

[20] H. E. J. Veeger, B. Yu, K. N. An, and R. H. Rozendal, "Parameters for modeling the upper extremity," *J. Biomech.*, vol. 30, no. 6, pp. 647–652, 1997, doi: 10.1016/S0021-9290(97)00011-0.

[21] N. Bogduk, G. Johnson, and D. Spalding, "The morphology and biomechanics of latissimus dorsi," *Clin. Biomech.*, vol. 13, no. 6, pp. 377–385, 1998, doi: 10.1016/S0268-0033(98)00102-8.

[22] R. L. Lieber, B. M. Fazeli, and M. J. Botte, "Architecture of selected wrist flexor and extensor muscles," *J. Hand Surg.*, vol. 15, no. 2, pp. 244–250, 1990, doi: 10.1016/0363-5023(90)90103-X.

[23] G. R. Johnson, D. Spalding, A. Nowitzke, and N. Bogduk, "Modelling the muscles of the scapula morphometric and coordinate data and functional implications," *J. Biomech.*, vol. 29, no. 8, pp. 1039–1051, 1996, doi: 10.1016/0021-9290(95)00176-X.

[24] F. C. T. Van der Helm, H. E. J. Veeger, G. M. Pronk, L. H. V. Van der Woude, and R. H. Rozendal, "Geometry parameters for musculoskeletal modelling of the shoulder system," *J. Biomech.*, vol. 25, no. 2, pp. 129–144, 1992, doi: 10.1016/0021-9290(92)90270-B.

[25] K. R. S. Holzbaur, W. M. Murray, and S. L. Delp, "A model of the upper extremity for simulating musculoskeletal surgery and analyzing neuromuscular control," *Ann. Biomed. Eng.*, vol. 33, no. 6, pp. 829–840, Jun. 2005, doi: 10.1007/s10439-005-3320-7.

[26] J. Langenderfer, S. A. Jerabek, V. B. Thangamani, J. E. Kuhn, and R. E. Hughes, "Musculoskeletal parameters of muscles crossing the shoulder and elbow and the effect of sarcomere length sample size on estimation of optimal muscle length," *Clin. Biomech.*, vol. 19, no. 7, pp. 664–670, Aug. 2004, doi: 10.1016/j.clinbiomech.2004.04.009.

[27] J. H. Petajan, "AAEM minimonograph #3: Motor unit recruitment," *Muscle Nerve*, vol. 14, no. 6, pp. 489–502, Jun. 1991, doi: 10.1002/mus.880140602.

[28] C. S. Bickel, C. M. Gregory, and J. C. Dean, "Motor unit recruitment during neuromuscular electrical stimulation: A critical appraisal," *Eur. J. Appl. Physiol.*, vol. 111, no. 10, pp. 2399–2407, Oct. 2011, doi: 10.1007/s00421-011-2128-4.

[29] B. I. Prilutsky and R. J. Gregor, "Analysis of muscle coordination strategies in cycling," *IEEE Trans. Rehabil. Eng.*, vol. 8, no. 3, pp. 362–370, Sep. 2000, doi: 10.1109/86.867878.

[30] J. Rasmussen, M. Damsgaard, and M. Voigt, "Muscle recruitment by the min/max criterion—A comparative numerical study," *J. Biomech.*, vol. 34, no. 3, pp. 409–415, 2001, doi: 10.1016/S0021-9290(00)00191-3.

[31] C. Quental, J. Folgado, and J. Ambrósio, "A window moving inverse dynamics optimization for biomechanics of motion," *Multibody Syst. Dyn.*, vol. 38, no. 2, pp. 157–171, Oct. 2016, doi: 10.1007/s11044-016-9529-4.

[32] A. A. Nikooyan, H. E. J. Veeger, E. K. J. Chadwick, M. Praagman, and F. C. T. van der Helm, "Development of a comprehensive musculoskeletal model of the shoulder and elbow," *Med. Biol. Eng. Comput.*, vol. 49, no. 12, pp. 1425–1435, Dec. 2011, doi: 10.1007/s11517-011-0839-7.

[33] R. H. Miller, "Hill-based muscle modeling," in *Handbook of Human Motion*. Cham, Switzerland: Springer, 2017, pp. 1–23, doi: 10.1007/978-3-319-30808-1_203-1.

[34] N. C. Silver and W. P. Dunlap, "Averaging correlation coefficients: Should Fisher's z transformation be used?" *J. Appl. Psychol.*, vol. 72, no. 1, pp. 146–148, 1987, doi: 10.1037/0021-9010.72.1.146.

[35] D. M. Corey, W. P. Dunlap, and M. J. Burke, "Averaging correlations: Expected values and bias in combined Pearson *rs* and Fisher's *z* transformations," *J. Gen. Psychol.*, vol. 125, no. 3, pp. 245–261, Jul. 1998, doi: 10.1080/00221309809595548.

[36] E. I. Obilor and E. C. Amadi, "Test for significance of Pearson's correlation coefficient (*r*)," *Int. J. Innov. Math. Stat. Energy Policies*, vol. 6, no. 1, pp. 11–23, 2018.

[37] E. S. Pearson, "The test of significance for the correlation coefficient," *J. Amer. Stat. Assoc.*, vol. 26, no. 174, pp. 128–134, Jun. 1931, doi: 10.1080/01621459.1931.10503208.

[38] D. J. Wilson, "The harmonic mean p-value for combining dependent tests," *Proc. Nat. Acad. Sci. USA*, vol. 116, no. 4, pp. 1195–1200, Jan. 2019, doi: 10.1073/pnas.1814092116.

[39] C. Klemt, D. Nolte, Z. Ding, L. Rane, R. A. Quest, M. E. Finnegan, M. Walker, P. Reilly, and A. M. J. Bull, "Anthropometric scaling of anatomical datasets for subject-specific musculoskeletal modelling of the shoulder," *Ann. Biomed. Eng.*, vol. 47, no. 4, pp. 924–936, Apr. 2019, doi: 10.1007/s10439-019-02207-2.

[40] W. Wu, P. V. S. Lee, A. L. Bryant, M. Galea, and D. C. Ackland, "Subject-specific musculoskeletal modeling in the evaluation of shoulder muscle and joint function," *J. Biomech.*, vol. 49, no. 15, pp. 3626–3634, Nov. 2016, doi: 10.1016/j.jbiomech.2016.09.025.
[41] A. A. Nikooyan, H. E. J. Veeger, P. Westerhoff, F. Graichen, G. Bergmann, and F. C. T. van der Helm, "Validation of the Delft shoulder and elbow model using *in-vivo* glenohumeral joint contact forces," *J. Biomech.*, vol. 43, no. 15, pp. 3007–3014, Nov. 2010, doi: 10.1016/j.jbiomech.2010.06.015.
[42] S. Martelli, H. E. J. Veeger, and F. C. T. V. Helm, "Scaling of a shoulder musculoskeletal model to individual subject data," *J. Biomech.*, vol. 40, no. 2, p. S68, 2007, doi: 10.1016/s0021-9290(07)70065-9.
[43] Q. Carlos, A. Margarida, A. Jorge, S. B. Goncalves, and F. João, "Influence of the musculotendon dynamics on the muscle force-sharing problem of the shoulder—A fully inverse dynamics approach," *J. Biomech. Eng.*, vol. 140, no. 7, Jul. 2018, Art. no. 071005, doi: 10.1115/1.4039675.
[44] T. S. Buchanan, D. G. Lloyd, K. Manal, and T. F. Besier, "Estimation of muscle forces and joint moments using a forward-inverse dynamics model," *Med. Sci. Sports Exerc.*, vol. 37, no. 11, pp. 1911–1916, Nov. 2005, doi: 10.1249/01.mss.0000176684.24008.6f.
[45] M. Cardona and C. E. G. Cena, "Biomechanical analysis of the lower limb: A full-body musculoskeletal model for muscle-driven simulation," *IEEE Access*, vol. 7, pp. 92709–92723, 2019, doi: 10.1109/ACCESS.2019.2927515.
[46] D. G. Lloyd and T. F. Besier, "An EMG-driven musculoskeletal model to estimate muscle forces and knee joint moments *in vivo*," *J. Biomech.*, vol. 36, no. 6, pp. 765–776, 2003, doi: 10.1016/S0021-9290(03)00010-1.
[47] I. W. Charlton and G. R. Johnson, "A model for the prediction of the forces at the glenohumeral joint," *Proc. Inst. Mech. Eng. H, J. Eng. Med.*, vol. 220, no. 8, pp. 801–812, Aug. 2006, doi: 10.1243/09544119JEIM147.

YOKHESH K. TAMILSELVAM received the master's degree in electrical engineering, with a focus on intelligent systems, from Clemson University, USA, in 2018. He is currently pursuing the Ph.D. degree in electrical engineering, with a focus on robotics, with the University of Western Ontario, Canada. His current work is related to the investigation of kinematics in movement disorder and improvements in therapy using rehabilitative robotics and machine learning techniques. In 2017, he had received training at Singapore University of Technology and Design and had published works related to the application of machine learning in robotics. His research interests include rehabilitation robotics, machine learning, biomechanics, control, and developing intelligent robot-assisted tools to investigate movement disorders

JACKY GANGULY received the M.D. degree (Hons.) and the D.M. degree in neurology from Medical College and Hospital, Kolkata. He then joined the Institute of Neurosciences, Kolkata (I-NK), as an Associate Consultant with the Department of Neurology. He is currently at the University of Western Ontario, Canada, and doing his clinical fellowship in Parkinson's disease and movement disorders. He has been trained in the clinical management of movement disorders like Parkinson's disease, atypical parkinsonism, ataxia, dystonia, myoclonus, tics, and chorea. Further, he also received training on botulinum toxin therapy in movement disorders and advanced therapies like deep brain stimulation (DBS), non-invasive transcranial electrical stimulation (tES), levodopa-carbidopa intestinal gel (LCIG)/duodopa, and apomorphine (subcutaneous and sublingual).

RAJNI V. PATEL (Life Fellow, IEEE) received the Ph.D. degree in electrical engineering from the University of Cambridge, U.K., in 1973, and currently holds the position of distinguished university professor and the Tier-1 Canada Research Chair with the Department of Electrical and Computer Engineering with cross-appointments with the Department of Surgery and the Department of Clinical Neurological Sciences, University of Western Ontario, London, ON, Canada. He is a Founding Member of the Canadian Surgical Technologies and Advanced Robotics (CSTAR) and serves as its Director of Engineering. He has over 35 years of research experience in the design, simulation, prototyping, and control of advanced robotic systems. Since 2000, his research interests include robotic and other mechatronic applications in minimally invasive surgery and therapy, haptics and teleoperation, surgical training and skills assessment, and more recently on applications of robotics and artificial intelligence for neurological movement disorders, including those due to Parkinson's disease and stroke. He is a fellow of the Royal Society of Canada, the Canadian Academy of Engineering, and ASME. He has served on the Editorial Boards of the IEEE TRANSACTIONS ON ROBOTICS, the IEEE/ASME TRANSACTIONS ON MECHATRONICS, the IEEE TRANSACTIONS ON AUTOMATIC CONTROL, *Automatica*, and the *Journal of Medical Robotics Research*. He is currently on the Editorial Board of *The International Journal of Medical Robotics and Computer Assisted Surgery*. He is an Editor of *The Encyclopedia of Medical Robotics: (In 4 Volumes) Volume 1: Minimally Invasive Surgical Robotics* (World Scientific Publishing Company, 2018).

MANDAR JOG (Member, IEEE) received the M.D. and FRCPC degrees. He is currently the Director of the National Parkinson Foundation Centre of Excellence in Parkinson's Disease and Movement Disorders Program at London Health Sciences Centre, London, ON, Canada, and a Professor of neurology at Western University, London. He is also one of the Associate Directors of Lawson Health Research Institute. The focus of his research projects include: speech, gait, balance, posture, tremor, and planning, and analysis of computational and mathematical modeling of these data. He was awarded the Dean's Award for Excellence in Research, in 2012; the Queens Diamond Jubilee Award, in 2013; and has been awarded the Faculty Scholar Award for exemplary research, teaching, and service, in 2014; the President's Award for Innovation from London Health Sciences Centre, in 2014; and the Strategic Research Fund Award from Lawson Health Research Institute, in 2015. He was awarded the Lawson Innovation Award for 2018.